Regularized Wulff Flows, Nonconvex Energies and Backwards Parabolic Equations

Thomas Cecil*, and Stanley Osher†

June 24, 2004

Abstract

In this paper we propose a method of regularizing the backwards parabolic partial differential equations that arise from using gradient descent to minimize surface energy integrals within a level set framework in 2 and 3 dimensions. The proposed regularization energy is a functional of the mean curvature of the surface. Our method uses a local level set technique to evolve the resulting fourth order PDEs in time. Numerical results are shown, indicating stability and convergence to the asymptotic Wulff shape.

1 Introduction

In the field of material science one often encounters laws governing the motion of the growth of crystals in $m = 2$ or 3 dimensions that take the form of

$$\min_{\Omega} \oint_{\partial\Omega} F(n) dS, \tag{1}$$

where n is the outward normal of the crystal boundary $\partial\Omega$ [16],[8]. If we embed the boundary $\partial\Omega = \Gamma$ as a level set of a function φ (we use the zero level set: $\{x|\varphi(x) = 0\}$), then (1) can be rewritten as [21]

$$\min_{\Omega} \int_{\mathbb{R}^m} F\left(\frac{\nabla\varphi}{|\nabla\varphi|}\right)\delta(\varphi)|\nabla\varphi| dx, \tag{2}$$

where δ is a distribution function, and we are assuming $\varphi < 0$ on the interior of Ω. Taking the Euler-Lagrange equation of (2) and employing the method of gradient descent we arrive at PDE of the form

$$\varphi_t = |\nabla\varphi|\left[\nabla \cdot DF\left(\frac{\nabla\varphi}{|\nabla\varphi|}\right)\right], \tag{3}$$

*Department of Mathematics, University of California, Los Angeles, CA 90095-1555, USA. email: tcecil@math.ucla.edu

†Department of Mathematics, University of California, Los Angeles, CA 90095-1555, USA. email: sjo@math.ucla.edu

where DF is the gradient of F with respect to its m arguments $\frac{\nabla\varphi}{|\nabla\varphi|}$. It is also common to examine the problem with an additional fixed volume constraint

$$\int_{\mathbb{R}^m} H(-\varphi)dx = V_0, \tag{4}$$

where H is the Heaviside function. With this additional constraint the problem posed is known a the Wulff problem [8].

Our goal is to evolve the second order time dependent PDE (3) to steady state, obtaining an equilibrium shape given by $\{x|\varphi(x) = 0\}$ that is the minimizing Wulff shape. However, for many physically meaningful energies F, (3) is backward parabolic and thus ill posed. Direct numerical solvers quickly exhibit unstable behavior for these types of problems. A proposed solution has been to add a regularizing term to the PDE which is derived by minimizing an additional energy term of the form

$$E_{reg} = \epsilon \int_{\mathbb{R}^m} g(k)\delta(\varphi)|\nabla\varphi|dx, \tag{5}$$

where k is the mean curvature of the interface, $g \geq 0$, is a convex function of φ, and ϵ is small [6],[10],[12],[4],[8],[7]. See also [5] for another method of treating (3) in the nonconvex case. In [9] the authors present a similar energy to (5) for $m = 3$ that is a functional of the curvature tensor. This minimization by gradient descent results in a fourth order time dependent parabolic PDE, including terms involving the surface Laplacian of curvature, $\Delta_s k$.

Adding these terms to a problem involving surface motion generally results in an equation consisting of first or second order derivatives governing the surface advection along with fourth order derivatives found in the regularization term. As these problems are nonlinear, an explicit numerical evolution is usually used. However, because the regularization coefficient ϵ will be chosen to be small ($O(dx^2)$), the fourth order restriction on the CFL condition for the regularization PDE that would normally yield a timestep of $dt \leq Cdx^4$ is reduced to $dt \leq Cdx^2$.

There has been work done in the way of numerical solutions of the regularization PDE without the backwards parabolic part, but there are few analytic results. In [3] the authors demonstrate many of the difficulties involved in modeling surface diffusion with an explicit scheme, the most serious of which is the time step restriction. Thus the attempts at numerical solutions are generally aimed at reducing the CFL condition as the fourth order restriction makes it intractable. In [18] a semi-implicit splitting method was used to make the CFL condition second order, but at the same time reducing the spatial accuracy to first order. In [20] the authors used a coupled system of second order PDEs to smooth normals of a surface, but their method is not a true energy minimization of (5). See also [11] for a physical simulation, [1] for anisotropic surface diffusion simulations, and [2] for an overview of the subject.

In this paper we solve (3) by adding a regularization of the form (5), with $g(k) = k^2$. The backwards parabolic fourth order PDE resulting from gradient descent is evolved in a local level set setting, using explicit finite difference

methods developed for Hamilton-Jacobi equations. Given a familiarity with level set evolutions on uniform grids, the resulting method is straightforward to implement. The applications of computable "curve lengthening" PDEs extend beyond crystal growth to image processing and other areas where corner sharpening is needed.

After explaining the equations we will discuss the numerical implementation and show computed results. In both 2d and 3d the equilibrium shapes we obtain approach the analytically predicted Wulff shapes. There have been studies done showing in 2d that the asymptotic solution to the regularized problem approaches the Wulff shape as $\epsilon \to 0$ [10],[19], but these analyses have not been extended to 3d as of yet. As far as we know these are the first 3d examples of nonconvex Wulff energy evolutions.

2 Two Dimensional Case

In 2 dimensions (1) can take the form of

$$\min_{\Omega} \oint_{\partial\Omega} \gamma(\theta) dS, \tag{6}$$

where θ is the angle of the normal of the crystal boundary $\partial\Omega$ with respect to some fixed vector [16],[8], e.g. $\theta(\varphi) \equiv \arctan(\frac{\varphi_y}{\varphi_x})$, defined appropriately on $[0, 2\pi)$. If we embed the boundary $\partial\Omega = \Gamma$ as a level set of a function φ, then the equation governing the motion of $\partial\Omega$ is

$$\varphi_t = (\gamma(\theta) + \gamma''(\theta))k, \tag{7}$$

where

$$k = \nabla \cdot \frac{\nabla\varphi}{|\nabla\varphi|}$$

which is the curvature of the interface, see [16] for a derivation of the Euler-Lagrange equation.

The PDE is ill posed when $\gamma(\theta) + \gamma''(\theta) < 0$. It is known that [8] one can convexify γ in a natural way that will make $\gamma(\theta) + \gamma''(\theta) \geq 0$. This is known as the Frank convexification of the Wulff problem defined by (6). When we add an additional constraint to (7) such that

$$\text{area}(\Omega) = C,$$

where C is a fixed constant, then the rescaled asymptotic solution of (3) is believed to be the same as the asymptotic solution of the convexified version of (3).

For example, if the surface tension is given by

$$\gamma(\theta) = 1 + |\sin(2\theta)|,$$

we can see that

$$\gamma(\theta)+\gamma''(\theta)=\begin{cases} 1-3\sin(2\theta), & \text{for } \theta\in[0,\pi/2]\cup[\pi,3\pi/2] \\ 1+3\sin(2\theta), & \text{for } \theta\in[\pi/2,\pi]\cup[3\pi/2,2\pi], \end{cases}$$

which changes sign. The Frank convexification is

$$\hat{\gamma}(\theta)=|\cos(\theta)|+|\sin(\theta)|,$$

so

$$\hat{\gamma}(\theta)+\hat{\gamma}''(\theta)=\sum_{i=0}^{3}\delta(\theta-i\pi/2)\geq 0$$

where $\delta(x)$ is a distribution function.

The asymptotic shape these surface evolutions yield is a square, but if we were to numerically evolve the PDE given in (7) using γ we would quickly see a blowup in the solution at all points where $\gamma+\gamma''<0$. Even the evolution using $\hat{\gamma}$ would require some delicacy as the CFL condition would be restricted by the magnitude of $\delta\, k$, which could become very large if $|\theta-i\pi/2|\approx 0$ near corners of Γ.

The regularized energy we minimize is

$$\min_{\varphi}\int_{\mathbb{R}^2}[\gamma(\theta(\varphi))+\epsilon k^2]\delta(\varphi)|\nabla\varphi|dx \tag{8}$$

Using gradient descent the resulting evolution PDE is

$$\varphi_t=\{[\gamma(\theta(\varphi))+\gamma''(\theta(\varphi))]k-\epsilon(2\Delta_s k+k^3)\}|\nabla\varphi|. \tag{9}$$

In order to allow all level sets to move we have replaced the $\delta(\varphi)$ function in front of all terms and replaced it with $|\nabla\varphi|$ which has now become a standard practice, see e.g. [21]. The definitions for k and $\Delta_s k$ are as follows

$$k\equiv\Bigg[\sum_{i=1}^{Ndim}\varphi_{x_ix_i}\Bigg(\sum_{\substack{j=1\\ j\neq i}}^{Ndim}\varphi_{x_j}^2\Bigg)-\sum_{i=1}^{Ndim}\sum_{\substack{j=1\\ j\neq i}}^{Ndim}\varphi_{x_ix_j}\varphi_{x_i}\varphi_{x_j}\Bigg]/|\nabla\varphi|^3, \tag{10}$$

$$\begin{aligned}\Delta_s k\equiv div_s(\nabla_s k)&=\text{trace}(P\nabla(P\nabla k))) \\ &=\frac{1}{|\nabla\varphi|^2}\Bigg[\sum_{i=1}^{Ndim}k_{x_ix_i}\Bigg(\sum_{\substack{j=1\\ j\neq i}}^{Ndim}\varphi_{x_j}^2\Bigg)-\sum_{i=1}^{Ndim}\sum_{\substack{j=1\\ j\neq i}}^{Ndim}k_{x_ix_j}\varphi_{x_i}\varphi_{x_j}\Bigg] \\ &\quad-\frac{k}{|\nabla\varphi|}\Bigg[\sum_{i=1}^{Ndim}k_{x_i}\varphi_{x_i}\Bigg],\end{aligned} \tag{11}$$

where $P=I-n\otimes n,\ n=\nabla\varphi/|\nabla\varphi|,\ Ndim=2$. The matrix P is a projection onto the surface with normal n. See [9], [18] for derivations of the above formulas.

3 Three Dimensional Case

In 3 dimensions (1) may take the form of

$$\min_{\Omega} \oint_{\partial\Omega} \gamma(\theta,\omega) dS, \tag{12}$$

where θ, ω are a spherical coordinate parameterization of the angles of the normal of the crystal boundary $\partial\Omega$,

$$\omega = \tan^{-1}\left(\frac{W_3}{\sqrt{W_1^2+W_2^2}}\right),\ \theta = \tan^{-1}\left(\frac{W_2}{W_1}\right), \tag{13}$$

where $W = \nabla\varphi/|\nabla\varphi|$. If we embed the boundary $\partial\Omega = \Gamma$ as the 0 level set of a function φ, then (12) becomes

$$\min_{\varphi} \int_{\mathbb{R}^3} \gamma(\theta,\omega)|\nabla\varphi|\delta(\varphi)dx, \tag{14}$$

using gradient descent on this energy we can derive the equation governing the motion of $\partial\Omega$ as

$$\begin{aligned} \varphi_t \quad &= |\nabla\varphi|\nabla\cdot\left\{ \quad \gamma\frac{\nabla\varphi}{|\nabla\varphi|} \right. && \text{(15a)}\\ &\qquad +\gamma_\theta|\nabla\varphi|\left[\frac{-\varphi_y}{\varphi_x^2+\varphi_y^2}, \frac{\varphi_x}{\varphi_x^2+\varphi_y^2}, 0\right] \\ &\qquad \left. +\gamma_\omega\left[\frac{-\varphi_x\varphi_z}{|\nabla\varphi|\sqrt{\varphi_x^2+\varphi_y^2}}, \frac{-\varphi_y\varphi_z}{|\nabla\varphi|\sqrt{\varphi_x^2+\varphi_y^2}}, \frac{\sqrt{\varphi_x^2+\varphi_y^2}}{|\nabla\varphi|}\right]\right\}. \end{aligned}$$

Again we note that the $\delta(\varphi)$ has been replaced with $|\nabla\varphi|$. It can be shown that if $\varphi_z = 0$ and $\gamma_\omega = 0$ then we recover the 2d PDE (7). So the examples from section 2 showing ill posedness can also be applied here.

The regularization energy we add is the same as in the 2d case, but in the 3d case k is the total (twice the mean) curvature. In the PDE resulting from gradient descent on this energy, instead of the $-\epsilon(2\Delta_s k + k^3)|\nabla\varphi|$ term that was added to the right side of (9) we will evolve (15a), with an extra regularization term on the right hand side given by

$$-\epsilon|\nabla\varphi|(2\Delta_s k + 2k|L|^2 - k^3), \tag{15b}$$

where $L = \nabla_s n = JP$, with $J_{i,j} = \partial n_i/\partial x_j$, P is the projection matrix described above, and

$$|L|^2 = L\cdot L = \sum_{i=1}^{Ndim}\sum_{j=1}^{Ndim} L_{i,j}^2. \tag{16}$$

Level set representations of k, $\Delta_s k$ can be found by taking (10), (11), respectively with $Ndim = 3$. Note that in 2d we have $|L|^2 = k^2$ so that the regularization PDE terms in (15b) are the same as those in (9). See [9], for a further discussion of this formula.

4 Numerical Methods

The computational domains are discretized using a uniform rectangular grid. We evolve the PDEs in time using the method of lines. We treat the evolutions (9), (15) as a Hamilton-Jacobi problems of the form

$$\varphi_t + V_n|\nabla\varphi| = 0.$$

All of the derivatives within each V_n that are shown in (9), (15b), and using (10), (11), and (16) are calculated using central finite differencing.

For the V_n terms in (15a) we leave V_n in divergence form. This is done because for many common energy terms, γ, the second partials with respect to θ, ω involve delta functions. By leaving the terms in divergence form we allow the numerical discretization to resolve these singularities rather than attempting to approximate them explicitly.

To calculate the partial derivatives at a point x_0 we use finite differencing using points offset from x_0 by half a grid cell depending on the direction in which the divergence is being taken. For example in 2d if we are calculating $\nabla \cdot u_{i,j}$, then when taking the x direction of the divergence we use $\partial u_{i,j}/\partial x \approx (u_{i+1/2,j} - u_{i-1/2,j})/dx$, where the partial derivative terms that make up u are calculated by central finite differencing (again using values offset by half a grid cell). So continuing with our example, if $u \equiv v_x v_y$, then we would use

$$\frac{\partial v_{i+1/2,j}}{\partial x} \approx \frac{v_{i+1,j} - v_{i,j}}{dx},$$

$$\frac{\partial v_{i+1/2,j}}{\partial y} \approx \frac{1}{4}\frac{\sum_{k1=0}^{1}\sum_{k2=0}^{1} v_{i+k1,j+k2} - \sum_{k1=0}^{1}\sum_{k2=-1}^{0} v_{i+k1,j+k2}}{dy},$$

and there would be similar equations for $\partial v_{i-1/2,j}/\partial x$, $\partial v_{i-1/2,j}/\partial y$. This finite differencing procedure is done to ensure more compact stencils.

After taking finding V_n, we can use central differencing to calculate $|\nabla\varphi|$.

Time advancement is done using second order TVD Runge-Kutta solvers [13]. The time step restriction we use is $dt = 0.1dx^4/\epsilon$. Because of the backwards parabolic nature of the PDEs there are no theoretical or experimental estimates for time step restrictions on these types of problems.

The asymptotic limit of the convexified versions of these equations is for the interface to shrink to a Wulff shape and then vanish. Although the nonconvex case has not been studied as thoroughly, in certain examples we use a projected gradient method [17],[14],[21] to ensure that volume remains fixed in time. This is done by requiring that

$$\left| \int H(-\varphi)dx - V_0 \right| < \varepsilon \tag{17}$$

at any given time step, where H is a Heaviside function. Numerically this is done by first finding the current volume $V = \int H(-\varphi)dx$ using a smoothed approximation of H. We then attempt to find a constant λ such that

$$\int H(-\varphi + \lambda)dx = V_0.$$

Taking a first order approximation we find that

$$\int H(-\varphi + \lambda)dx \approx \int H(-\varphi) - \lambda\delta(-\varphi)|\nabla(-\varphi)|dx = V - \lambda S,$$

where S is the surface area of the interface. Solving for λ yields $\lambda = \frac{V-V_0}{S}$. We then adjust φ globally by adding λ to it at every point. Additional repetitions of this procedure can be done until (17) is satisfied, although in practice one step is usually enough. See [14] for a similar procedure.

The entire calculation is done within a local level set framework [15], involving only grid cells within tubes of a specified distance of the interface. This requires reinitialization of φ to a signed distance function when the interface has moved close to the boundary of the tubes, or $|\nabla\varphi|$ has moved far from 1. The reinitialization is done for all grid points in the computational domain.

5 Numerical Experiments

In this section we show numerical results of the problems P2D and P3D evolved to a steady state solution. In practice we use $\epsilon = 0.5dx^2$ for the regularization coefficient. If a fixed volume condition is imposed it will be noted in the specific example. The problems are solved on a uniform grid that discretizes the space $[-1, 1]^m$ in m dimensions. The spatial step size in each direction is $1/25$. Neumann BCs, $\partial\varphi/\partial n = 0$, are used.

First we show an accuracy calculation for a circle moving under backwards curvature flow i.e. $\gamma = -1$ in table 1. The circle is initialized with radius 0.4. The exact solution at time T is a circle with radius

$$r(T) = \sqrt{2T + (0.4)^2}.$$

The radius of the computed solution is measured along the x-axis.

T	$r(T)$ exact	$r(T)$ computed	error
0	0.4	-	-
0.0168	0.44	0.4415	0.0015
0.0352	0.48	0.4827	0.0027
0.0552	0.52	0.5290	0.0090

Table 1: Error for circle moving with backward curvature, $\gamma = -1$.

Figure 1 shows multiple time plots of an interface that is initialized as a square, evolving under backwards curvature flow, i.e. under the surface energy where $\gamma(\theta) = -1$.

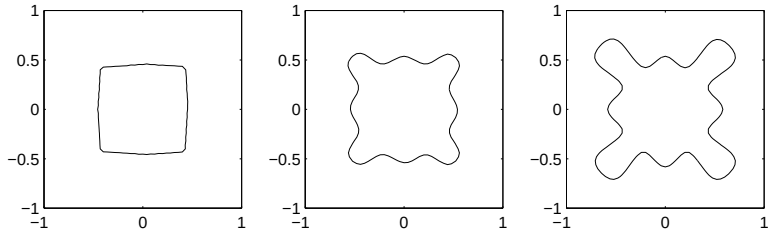

Figure 1: Backwards curvature flow, $\gamma(\theta) = -1$, at $t = 0, 0.08, 0.11$.

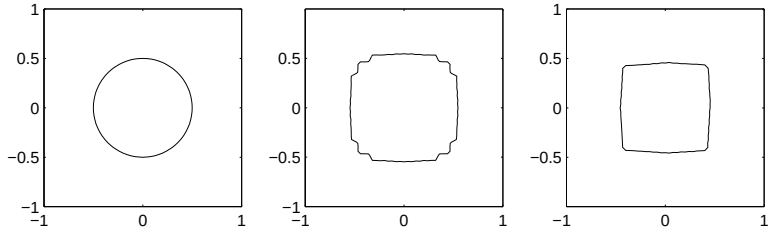

Figure 2: Evolution with surface energy defined by $\gamma(\theta) = 1 + 3|\sin(2\theta)|$, at $t = 0, 0.016, 0.08$.

Figure 2 shows an evolution with

$$\gamma(\theta) = 1 + 3|\sin(2\theta)|.$$

The asymptotic Wulff shape is a square. In this example volume preservation is enforced.

Figure 3 shows an evolution with

$$\gamma(\theta) = 1 + 3|\sin(1.5\theta)|.$$

The asymptotic Wulff shape is a triangle.

In 3 dimensions we show the evolution of an initial sphere under different surface energies. The surface energy density for figure 4 is

$$\gamma(\theta, \omega) = (1 + 3|\sin(1.5(\theta - \pi/4))|)(1 + 3|\cos(2\omega)|). \tag{18}$$

The energy density for figure 5 is

$$\gamma(\theta, \omega) = (1 + 3|\sin(2\theta)|)(1 + 3|\sin(2\omega)|). \tag{19}$$

6 Conclusion

In this paper we have implemented PDEs in two and three dimensions that regularize the backwards parabolic evolutions resulting from using the method

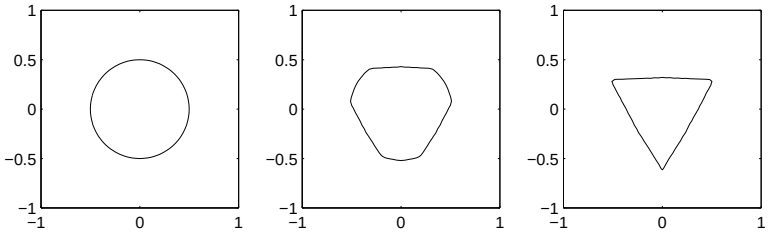

Figure 3: Evolution with surface energy defined by $\gamma(\theta) = 1 + 3|\sin(1.5\theta)|$, at $t = 0, 0.016, 0.064$.

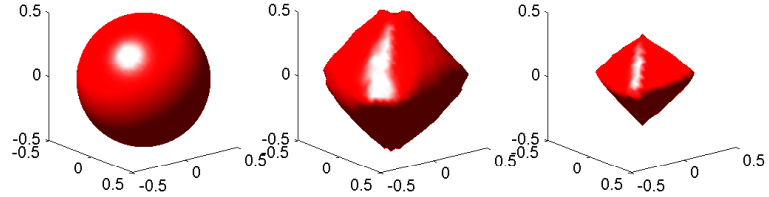

Figure 4: Evolution with surface energy defined using $\gamma(\theta, \omega) = ((1 + 3|\sin(1.5(\theta - \pi/4))|)(1 + 3|\cos(2\omega)|)$. At $t = 0, 0.016, 0.08$.

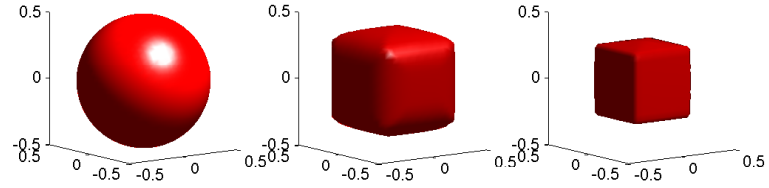

Figure 5: Evolution with surface energy defined using $\gamma(\theta, \omega) = (1 + 3|\sin(2\theta)|)(1 + 3|\sin(2\omega)|)$. At $t = 0, 0.0168, 0.036$.

of gradient descent to minimize surface energy integrals in a level set framework. Given a level set function φ, the regularization is based on minimizing a surface energy that is a functional of mean curvature, k.

Results indicate that our solutions are converging to the expected asymptotic Wulff shapes. For the case of a circle evolving under backwards mean curvature we have first order convergence to the analytic solution.

There is still work to be done concerning the analysis of the regularized equation in two and three dimensions. Areas to be studied include the asymptotic solution properties, the stability and convergence of the time dependent flow, and analysis of the numerical methods used to evolve the interface.

Acknowledgment: This work is supported by NSF grants DMS-0312222 and ACI-0321917. We would also like to thank Luminita Vese, Martin Burger, and Peter Smereka for interesting conversations regarding this topic.

References

[1] Martin Burger. Numerical simulation of anisotropic surface diffusion with curvature-dependent energy. *UCLA CAM Report 04-06*, February 2004.

[2] J.W. Cahn and J.E. Taylor. *Acta metall. mater.*, 42, 1994.

[3] David L. Chopp and J. A. Sethian. Motion by intrinsic Laplacian of curvature. *Interfaces Free Bound.*, 1(1):107–123, 1999.

[4] Antonio Di Carlo, Morton E. Gurtin, and Paolo Podio-Guidugli. A regularized equation for anisotropic motion-by-curvature. *SIAM J. Appl. Math.*, 52(4), 1992.

[5] Francesca Fierro, Roberta Goglione, and Maurizio Paolini. Numerical simulations of mean curvature flow in the presence of a nonconvex anisotropy. *Math. Models Methods Appl. Sci.*, 8(4):573–601, 1998.

[6] J.W. Gibbs. On the equilibrium of heterogeneous substances. *Trans. Conn. Acad.*, 1876,1878. Reprinted in The Scientific Papers of J.Willard Gibbs, Vol. 1, Dover, New York, 1961.

[7] A. A. Golovin, S. H. Davis, and A. A. Nepomnyashchy. A convective Cahn-Hilliard model for the formation of facets and corners in crystal growth. *Phys. D*, 122(1-4):202–230, 1998.

[8] Morton Gurtin. *Thermodynamics of Evolving Phase Boundaries in the Plane*. Springer Verlag, 1993.

[9] Morton E. Gurtin and Michel E. Jabbour. Interface evolution in three dimensions with curvature-dependent energy and surface diffusion: interface-controlled evolution, phase transitions, epitaxial growth of elastic films. *Arch. Ration. Mech. Anal.*, 163(3):171–208, 2002.

[10] C. Herring. Some theorems on the free energies of crystal surfaces. 82(1), 1951.

[11] M. Khenner, A. Averbuch, M. Israeli, and M. Nathan. Numerical simulation of grain boundary grooving by level set method. *J. Comput. Phys.*, 170:764–784, 2001.

[12] W.W. Mullins. *J. Appl. Phys.*, 28, 1957.

[13] Stanley Osher and Ronald P. Fedkiw. *Level Set Methods and Dynamic Implicit Surfaces*. Oxford Univ. Press, 2002.

[14] Stanley J. Osher and Fadil Santosa. Level set methods for optimization problems involving geometry and constraints. I. Frequencies of a two-density inhomogeneous drum. *J. Comput. Phys.*, 171(1):272–288, 2001.

[15] Danping Peng, Barry Merriman, Stanley Osher, Hongkai Zhao, and Myungjoo Kang. A PDE-based fast local level set method. *J. Comput. Phys.*, 155(2):410–438, 1999.

[16] Danping Peng, Stanley Osher, Barry Merriman, and Hong-Kai Zhao. The geometry of Wulff crystal shapes and its relations with Riemann problems. In *Nonlinear partial differential equations (Evanston, IL, 1998)*, volume 238 of *Contemp. Math.*, pages 251–303. Amer. Math. Soc., Providence, RI, 1999.

[17] J. B. Rosen. The gradient projection method for nonlinear programming. II. Nonlinear constraints. *J. Soc. Indust. Appl. Math.*, 9:514–532, 1961.

[18] Peter Smereka. Semi-implicit level set methods for curvature and surface diffusion motion. *J. Sci. Comp.*, 19(1–3):439–456, 2003.

[19] B. Spencer. Asymptotic solutions for the equilibrium crystal shape with small corner energy regularization. *Phys. Rev. E.*, to appear.

[20] T. Tasdizen, R. Whitaker, P. Burchard, and S. Osher. Geometric surface smoothing via anisotropic diffusion of normals. *UCLA CAM Report*, October 2002.

[21] Hong-Kai Zhao, T. Chan, B. Merriman, and S. Osher. A variational level set approach to multiphase motion. *J. Comput. Phys.*, 127(1):179–195, 1996.